Published online 16 May 2017 *Nucleic Acids Research, 2017, Vol. 45, No. 11* **6613–6627**
doi: 10.1093/nar/gkx417

Phosphorylation of the transcriptional repressor MYB15 by mitogen-activated protein kinase 6 is required for freezing tolerance in *Arabidopsis*

Sun Ho Kim[1], Ho Soo Kim[2], Sunghwa Bahk[1], Jonguk An[1], Yeji Yoo[1], Jae-Yean Kim[1] and Woo Sik Chung[1,*]

[1]Division of Applied Life Science (BK21 plus program), Plant Molecular Biology and Biotechnology Research Center, Gyeongsang National University, Jinju 52828, Korea and [2]Plant Systems Engineering Research Center, Korea Research Institute of Bioscience and Biotechnology, Daejeon 34141, Korea

Received January 9, 2017; Revised April 25, 2017; Editorial Decision April 26, 2017; Accepted May 15, 2017

ABSTRACT

The expression of *CBF* (C-repeat-binding factor) genes is required for freezing tolerance in *Arabidopsis thaliana*. *CBFs* are positively regulated by INDUCER OF CBF EXPRESSION1 (ICE1) and negatively regulated by MYB15. These transcription factors directly interact with specific elements in the *CBF* promoters. Mitogen-activated protein kinase (MAPK/MPK) cascades function upstream to regulate *CBFs*. However, the mechanism by which MPKs control *CBF* expression during cold stress signaling remains unknown. This study showed that the activity of MYB15, a transcriptional repressor of cold signaling, is regulated by MPK6-mediated phosphorylation. MYB15 specifically interacts with MPK6, and MPK6 phosphorylates MYB15 on Ser168. MPK6-induced phosphorylation reduced the affinity of MYB15 binding to the *CBF3* promoter and mutation of its phosphorylation site (MYB15^{S168A}) enhanced the transcriptional repression of *CBF3* by MYB15. Furthermore, transgenic plants overexpressing MYB15^{S168A} showed significantly reduced *CBF* transcript levels in response to cold stress, compared with plants overexpressing MYB15. The *MYB15*^{S168A}-overexpressing plants were also more sensitive to freezing than *MYB15*-overexpressing plants. These results suggest that MPK6-mediated regulation of MYB15 plays an important role in cold stress signaling in *Arabidopsis*.

INTRODUCTION

Cold temperatures and freezing can adversely affect plant growth and development, thus limiting the geographical distribution of plants and decreasing agricultural yields. However, plants can acclimate to low temperatures via the reprogramming of gene expression, metabolism and cellular architecture (1,2). Most of our current knowledge on cold sensing and acclimation mechanisms comes from studies of the model plant *Arabidopsis thaliana* (3,4). Evidence suggests that cold stress is sensed through cold-induced changes in membrane fluidity and other signals, which induce fluxes in cytoplasmic Ca^{2+} currents. These Ca^{2+} fluxes activate kinases or kinase cascades, leading to the transcription of cold regulated (*COR*) genes, which are required for freezing tolerance.

Members of the C-repeat (CRT)-binding factor (CBF) family of transcription factors (also known as dehydration-responsive element-binding protein 1 family members, DREB1s) have central functions in the regulation of cold stress-induced transcription. The expression levels of *CBFs* determine the levels of *COR* gene expression and freezing tolerance (5,6). The transcription of *CBFs* is activated by INDUCER OF CBF EXPRESSION1 (ICE1) and ICE1-like transcription factors (MYC-family transcription factors) and repressed by MYB15 (an MYB family transcription factor), which bind to specific elements in the *CBF* promoters.

Forward and reverse genetic approaches have demonstrated that mitogen-activated protein kinase (MAPK/MPK) cascades regulate *CBF* gene expression. However, the molecular links connecting cold-responsive MPK cascades and *CBF* gene transcription remain to be identified. In eukaryotes, MPK cascades play essential roles in transmitting stimuli from mitogens, developmental cues and various environmental stresses (7,8). MPK cascades are major signaling pathways that function downstream of sensors/receptors that are positively or negatively regulated by cytosolic Ca^{2+} influx in a tissue-specific manner (9). MPK cascades consist of three sequentially acting protein kinases. Signal transduction via MPK cascades is initiated by the activation of MPK

*To whom correspondence should be addressed. Tel: +82 55 772 1363; Fax: +82 55 759 9363; Email: chungws@gnu.ac.kr

kinase kinase (MAPKKK/MEKK/MTK/MKKK). This enzyme phosphorylates and activates MPK kinase (MAPKK/MEK/MKK), which in turn phosphorylates and activates MPK. MKKKs are serine (Ser, S)/threonine (Thr, T) kinases that phosphorylate Ser/Thr on conserved S/T-X_{3-5}-S/T motifs of the MKK activation loop (10). MKKs are dual-specificity kinases that doubly phosphorylate the T-X-Y motif in the activation loop of MPKs (10). The terminal kinases of the cascade, MPKs, are also Ser/Thr kinases. The substrates of MPKs include other kinases and various transcription factors.

The *Arabidopsis thaliana* genome encodes 20 predicted MPKs, which differ in the signature sequences of their activation loops (8,11). Of these, MPK3, MPK4 and MPK6, the most extensively studied MPKs, are activated by stress (pathogens, osmotic, cold and oxidative stress), developmental cues and auxin signaling (12–14). Each MPK is thought to participate in responses to a specific stress or a subset of stresses. The specificity of their activity appears to be determined by unique MKK-MPK combinations that participate in the responses to different stresses. For example, drought and wounding induce the MKK1-MPK4 module, abscisic acid activates MKK1-MPK3 and osmotic shock activates MKK1-MPK3/MPK6 (4,15–17). The MEKK1-MKK2-MPK4/MPK6 cascade plays an important role in the cold signal transduction pathway (4). MKK2 is specifically activated by cold stress in *Arabidopsis* protoplasts. Yeast two-hybrid analyses, as well as *in vitro* and *in vivo* protein kinase assays, showed that MKK2 phosphorylates MPK4 and MPK6. Transgenic plants overexpressing MKK2 exhibit constitutive MPK4 and MPK6 activity and improved freezing tolerance through increased expression of *CBF* genes (4).

The specificity of the response to a given stimulus could also be determined by the choice of MPK substrates. Several studies have attempted to identify the substrates and interaction partners of MPKs (18,19). Protein microarray analysis of 1690 unique *Arabidopsis thaliana* proteins identified 39 proteins as substrates of MPK6 and 48 proteins as substrates of MPK3 (20). Another protein microarray experiment identified the substrates of 10 different activated MPKs (21). More studies will be required to establish that these candidates truly function as MPK substrates. In addition, each candidate must still be connected to specific signaling outcomes.

Downstream components of the cold-responsive MPK cascade, such as MPK4 and MPK6 substrates, remain to be identified. The transcription factor MYB15 was revealed as an MPK6 interaction partner by yeast two-hybrid analysis of an *Arabidopsis* transcription factor library (22). Protein microarray analysis also predicted that MYB15 is phosphorylated by activated MPK6 and MPK10 (20). MYB15 represses *CBF* gene expression and freezing tolerance in *Arabidopsis* (23,24) and *MYB15* is expressed in *Arabidopsis* in the absence of cold stress. Mutational inactivation of *MYB15* results in enhanced expression of *CBFs* during cold acclimation and the freezing tolerance response, whereas overexpression of *MYB15* has the opposite effect. MYB15 binds to the conserved MYB transcription factor recognition sequences in the promoters of *CBFs* and inhibits their transcription.

In this study, we obtained several lines of evidence that MYB15 is a substrate for MPK6 both *in vitro* and *in vivo*. MYB15 physically interacted with MPK6 *in vitro* (in a yeast two-hybrid assay) and *in planta*, and MYB15 was phosphorylated by both recombinant and native MPK6. We identified an MPK6 phosphorylation site in MYB15 and performed mutational analysis showing that the binding affinity of MYB15 to the *CBF3* promoter fragment, as well as the effect of MYB15 on *CBF3* gene expression, are regulated by the phosphorylation status of the MPK6-target phosphorylation site. Comparison of the freezing tolerance of transgenic plants overexpressing native MYB15 or $MYB15^{S168A}$, a mutant MYB15 protein lacking the MPK6-phosphorylation site, demonstrated that an intact MPK6-target phosphorylation site is associated with freezing tolerance. The finding that transcriptional derepression of *CBF* genes and the freezing tolerance response are mediated by direct phosphorylation of MYB15 by MPK6 increases our understanding of the cold stress signaling pathway in *Arabidopsis*.

MATERIALS AND METHODS

Plant materials and growth conditions

The *Arabidopsis thaliana* lines used in this study were in the Columbia background. For surface sterilization, seeds were soaked for 1 min in 70% EtOH, followed by 10 min in 1/10-diluted commercial bleach (0.4% NaOCl) and three washes with sterile distilled water. Surface-sterilized seeds were sown on agar plates containing half-strength Murashige-Skoog (MS) salts and vitamins (25), 2.0% sucrose and 0.8% agar. The plates were incubated in the dark for 3 days at 4°C, followed by incubation at 22°C in a growth chamber under a 16 h light/8 h dark photoperiod. Ten- to twelve-day-old seedlings were transferred to soil and grown under the same conditions.

Nicotiana benthamiana seeds were sown in soil and grown in a growth chamber at 24°C under a 16 h light/8 h dark photoperiod. Seven-week-old *N. benthamiana* plants were used for *Agrobacterium*-mediated transient expression.

Plasmid construction, site-directed mutagenesis and expression of recombinant proteins

Full-length and partial open reading frames (ORFs) encoding the N-terminal (amino acids 1–172) and C-terminal (amino acids 173–285) regions of *MYB15* were amplified by polymerase chain reaction (PCR) from a cDNA library of *Arabidopsis* seedlings using gene-specific primers (Supplementary Table S1). The amplicons were cloned into the pGEM-T Easy Vector, and their fidelity was verified by sequencing. To create in-frame N-terminal GST fusions, the inserts were excised with BamHI and EcoRI and cloned into the pGEX 4T-1 vector (Amersham Biosciences, USA). Single amino acid substitutions in full-length GST-MYB15 (T18A, S168A and T18A/S168A) were produced using the primers listed in Supplementary Table S2 using a QuikChange Site-directed Mutagenesis kit (Stratagene, USA). The mutations were confirmed by sequencing. The GST-fusion constructs were transformed into BL21

(DE3) *Escherichia coli*, and GST fusion proteins were expressed and purified using glutathione Sepharose-4B beads according to the manufacturer's instructions (GE Healthcare, USA). To express His- or GST-tag-fused MPKs in bacteria, full-length *MPK3, MPK4* or *MPK6* ORFs were amplified by PCR from a cDNA library of *Arabidopsis* seedlings using gene-specific primers (Supplementary Table S2) and cloned into the pGEM-T Easy Vector (Promega, USA). Verified inserts by sequencing were excised with BamHI and SalI, and subcloned into pQE30 or pGEX 4T-1 for His- or GST-tag-fused MPKs, respectively. The His-fusion constructs were transformed into *E. coli* (M15), and His-tag fusion proteins were expressed and purified using Ni-NTA agarose beads according to the manufacturer's instructions (Qiagen, Germany).

In vitro pull-down assay

Pull-down assays were carried out to examine the interaction of MYB15 with MPK3, MPK4 or MPK6. GST-MYB15 and GST were immobilized by incubating crude proteins (100 μg) with 10 μl of glutathione-Sepharose 4B beads in 1 ml buffer (50 mM Tris–HCl, pH 7.5, 200 mM NaCl, 1% Triton X-100, 0.1 mM ethylenediaminetetraacetic acid (EDTA) and 0.5 mM DTT) for 4 h at 4°C. Glutathione-Sepharose 4B beads containing immobilized proteins were collected by centrifugation and incubated overnight at 4°C with purified His-MPK3, His-MPK4, or His-MPK6 (10 μg) in 1 ml binding buffer (50 mM Tris–Cl pH 7.5, 200 mM NaCl, 0.1 mM EDTA and 0.5 mM DTT). Beads were collected by centrifugation and washed three times with binding buffer at 4°C. Proteins were eluted by boiling in sodium dodecyl sulphate-polyacrylamide gel electrophoresis (SDS-PAGE) loading buffer, separated by 10% SDS-PAGE and transferred onto an Immobilon-P membrane for immunoblotting. His-tagged proteins were detected on the membrane with polyclonal anti-His antibodies (Abcam, UK) using the enhanced chemiluminescence (ECL) technique.

Yeast two-hybrid analysis

Full-length ORFS of *MYB15*, *MPK3*, *MPK4* and *MPK6* were amplified using gene-specific primers (Supplementary Tables S1 and 2) and cloned into pGAD424 (prey) and pAS2–1 (bait) vectors, respectively. Prey and bait plasmids were co-transformed into yeast strain pJ69–4A for interaction analysis, and colonies were selected after 2–3 days growth at 30°C on SD-Trp-Leu medium. The transformants were tested for positive bait–prey interactions by monitoring the activation of *ADE2* and *LacZ* reporter genes as described.

Luciferase complementation imaging assay

The luciferase (LUC) complementation imaging assay was performed as described by Chen *et al*. (26). Full-length *MPK6* and *MYB15* ORFs were inserted into pCAMBIA1300-NLuc and pCAMBIA1300-CLuc, resulting in the production of *CaMV35S*: *MPK6-NLuc* and *CaMV35S*: *CLuc-MYB15*, respectively. The constructs were mobilized into *Agrobacterium tumefaciens* strain GV3101 (pMP90) (27). The *Agrobacterium* cells were grown in LB medium at 28°C overnight, collected by centrifugation, resuspended in induction medium at 0.3 OD_{600nm} (28) and incubated for 8–12 h at 28°C with shaking. Bacteria were collected by centrifugation, washed once with infiltration buffer (10 mM $MgCl_2$, 10 mM MES and 100 mM acetosyringone) and resuspended in infiltration buffer at 0.5 OD_{600nm}. Bacterial suspensions were infiltrated into young, fully expanded leaves of 3-week-old *N. benthamiana* plants using a needleless syringe. After infiltration, the plants were immediately covered with plastic bags and incubated at 23°C for 3 days. The plastic bags were removed, and infiltrated leaves were sprayed with luciferin solution (100 μM D-luciferin and 0.01% Triton X-100) and incubated in the dark for 4 h to quench fluorescence. LUC activity was observed under a low-light EMCCD apparatus (AndoriXon; Andor, UK).

Mass spectrometric analysis of phosphopeptides using TiO_2 microcolumns

GST-MYB15 was treated with His-MPK6 as described below for the *in vitro* kinase assays. Protein bands were excised after resolution by SDS-PAGE and in-gel digested with modified trypsin (Promega, USA) (29). The digested peptides were dissolved in loading buffer (80% acetonitrile and 5% trifluoroacetic acid) and passed through a TiO_2 microcolumn (29). Phosphopeptides were eluted with NH_4OH (pH 10.5), applied to a Poros Oligo R3 column (Applied Biosystems, USA) and eluted from the column using 2,5-dihydroxybenzoic acid (DHB; Fluka, USA) solution (20 mg/ml DHB, 50% acetonitrile, 0.1% trifluoroacetic acid and 1% ortho-phosphoric acid). MALDI-MS analysis was performed using a Voyager-DE STR mass spectrometer (PerSeptive Biosystems Inc., USA). Mass spectra were obtained in the reflectron/delayed extraction mode. Monoisotopic peptide masses were analyzed using MoverZ software (www.proteometric.com).

In vitro and in-gel kinase assays

In vitro kinase reactions were performed in kinase buffer (25 mM Tris–HCl, pH 7.5, 1 mM DTT, 20 mM $MgCl_2$, 2 mM $MnCl_2$, and 50 μM [γ-^{32}P] ATP) containing GST-MPK6 or His-MPK6 (1 μg) and substrate in a total reaction volume of 20 μl. GST (1 μg; negative control), myelin basic protein MBP (0.5 μg; positive control) and GST-MYB15 variants (2 μg) were used as substrates. The reactions were initiated using 1 μCi [γ-^{32}P] ATP and allowed to proceed at 30°C for 30 min. The kinase reactions were stopped by adding 6 μl of 4 × SDS sample buffer and boiling for 5 min. Reaction products were resolved by 10% SDS-PAGE. The gels were autoradiographed and stained with Coomassie Brilliant Blue (CBB) R-250, using pre-stained markers to estimate protein size.

The in-gel kinase assay was performed using extracts from 2- to 3-week-old Petri dish-grown wild-type (WT), *mpk3* (Salk_127507) and *mpk6* mutant (Salk_127507) seedlings treated with cold (4°C) for the indicated times. The in-gel kinase assay was performed as described previously

with some modifications (30). In brief, cell-free extracts (30 μg total proteins) were incubated at 60°C for 10 min and separated by 10% SDS-PAGE on a separating gel embedded with 0.5 mg/ml purified GST-MYB15 as a kinase substrate. After electrophoresis, the gel was washed three times with washing buffer (25 mM Tris–HCl, pH 7.5, 0.5 mM DTT, 0.1 mM Na_3VO_4, 5 mM NaF, 0.5 mg/ml bovine serum albumin and 0.1% Triton X-100) to remove the SDS. The proteins were renatured by incubating the gel overnight at 4°C in renaturing buffer (25 mM Tris–HCl, pH 7.5, 1 mM DTT, 0.1 mM Na_3VO_4 and 5 mM NaF) with three changes of buffer. The gel was equilibrated in reaction buffer (25 mM Tris–HCl, pH 7.5, 2 mM EGTA, 12 mM $MgCl_2$, 1 mM DTT and 0.1 mM Na_3VO_4) at room temperature for 30 min. The phosphorylation reaction was carried out by incubating the gel at room temperature for 1.5 h in 20 ml of reaction buffer containing 0.5 μM ATP and 50 μCi [γ-^{32}P] ATP. The reaction was stopped by transferring the gel to stop solution (5% trichloroacetic acid and 1% disodium pyrophosphate). Gels were washed with stop solution for 5 h at room temperature with four changes of solution, dried on 3M paper and imaged using a Fuji Film FLA-5000 imaging system.

Electrophoretic mobility shift assay (EMSA)

The −984 to −785 bp region of the *CBF* promoter, which binds to MYB15 (23) and contains an MYB response element, was amplified by PCR from *Arabidopsis* genomic DNA, separated by agarose gel electrophoresis and recovered by elution using a gel purification kit (GeneAll, Korea). Eluted fragments were end-labeled with [γ-^{32}P] ATP and T_4 polynucleotide kinase. The DNA-binding reaction was performed at 25°C for 20 min in binding buffer (20 mM HEPES/KOH pH 7.9, 0.5 mM dithiothreitol, 0.1 mM EDTA, 50 mM KCl and 15% glycerol) containing 20 000 cpm of ^{32}P-labeled DNA probe, 1 μg poly (dI-dC) and 0.5 μg bacterially produced GST-MYB15 variants that had been phosphorylated (or not) by MPK6. For competition, purified protein was incubated with unlabeled probes for 30 min at 25°C, before incubating with the labeled probe. The reaction mixture was subjected to electrophoresis on a 5% polyacrylamide gel in 0.5 × Tris-Borate-EDTA (TBE) buffer at 80 V for 3 h. The gel was dried and mounted for autoradiography at −70°C with an intensifying screen.

Transient expression assay

The reporter plasmid was a pUC19-derived plasmid containing the β-glucuronidase (*GUS*) reporter gene under the control of a chimeric promoter containing a *CBF3* promoter region (−2000 to −1 bp) inserted in front of the *CaMV35S* minimal promoter (31). For effector plasmids, *MYB15* or *MYB15*^{S168A} ORFs were inserted into a plant expression vector (pHBT95) containing the *35S C4PPDK* promoter and *nos* terminator (32). A construct carrying the 35S promoter fused to the *LUC* gene was used as an internal control to normalize the variation in cell numbers, transformation efficiency and cell viability of each transfection (33). Transient expression of these constructs was performed as described previously (34). Protoplasts (2×10^6) were co-transfected with 20 μg plasmid DNA consisting of a mixture of reporter, effector and internal control constructs. The transfected protoplasts were incubated for 16 h in the dark at 22°C before GUS and LUC activity measurements. In each sample, the GUS activity of the cell lysate was divided by the LUC activity, thereby normalizing the data to control for variations in transfection efficiency.

Construction of transgenic plants

The *CaMV35S:3XFlag-MYB15* and *CaMV35S:3XFlag-MYB15*^{S168A} constructs in the binary vector pCAMBIA 1300 were introduced into *Agrobacterium* strain GV3101 (pMP90) and used to transform *Arabidopsis* plants by the floral dip method (35). Transformants were selected on MS medium containing 40 μg/ml hygromycin. T_3 homozygous progeny of transgenic plants expressing high levels of MYB15 were used for all experiments.

Extraction and immunoblot analysis of *Arabidopsis* proteins

Tissues were ground in liquid nitrogen and extracted in protein extraction buffer (50 mM HEPES, pH 7.5, 5 mM EDTA, 5 mM EGTA, 1 mM Na_3VO_4, 25 mM NaF, 50 mM-glycerophosphate, 2 mM DTT, 2 mM PMSF, 5% glycerol, 1% Triton X-100 and protease inhibitor). After two rounds of centrifugation at 12 000 × *g* for 10 min, the supernatants were transferred to clean tubes and stored at −80°C until use. Protein concentrations were determined using a Bio-Rad Protein Assay kit (Bio-Rad) with BSA as a standard. For immunoblot analysis, total protein was extracted from the leaves of 2-week-old plants and 30 μg protein samples were separated by 10% SDS-PAGE and transferred to PVDF membranes. Proteins were detected using mouse anti-Flag (1:5000; Sigma, USA) as a primary antibody and alkaline phosphate-conjugated anti-mouse as a secondary antibody (1:5000) and visualized using an ECL kit (Amersham Pharmacia Biotech, UK).

Quantitative RT-PCR

Total RNA was extracted using the LiCl/phenol method according to a published protocol (36), and 5 μg total RNA was reverse-transcribed in a 100-μl reaction volume using SuperScript II RNase-Reverse Transcriptase (Invitrogen, USA). Quantitative RT-PCR was performed in a 15 μl reaction volume containing 1 μl RT products, 10 pmole of gene-specific primers and 7.5 μl SsoFast EvaGreen Supermix (Bio-Rad, USA) using the CFX96 Real-Time System (Bio-Rad, USA). The reaction conditions included an initial 5 min pre-incubation at 94°C, 45 cycles of 94°C for 30 s, 55°C for 30 s and 72°C for 40 s followed by melting curves with 90 cycles at 55°C increasing 0.5°C/cycle and final cooling for 10 min at 72°C. Primers used for PCR are shown in Supplementary Table S2.

Ion leakage from leaves

Ion leakage tests were carried out as described by Ishitani *et al.* (37). Briefly, one excised leaf from a 3-week-old soil-grown plant was placed in a test tube containing 100 μl of deionized H_2O, which was transferred to a circulating

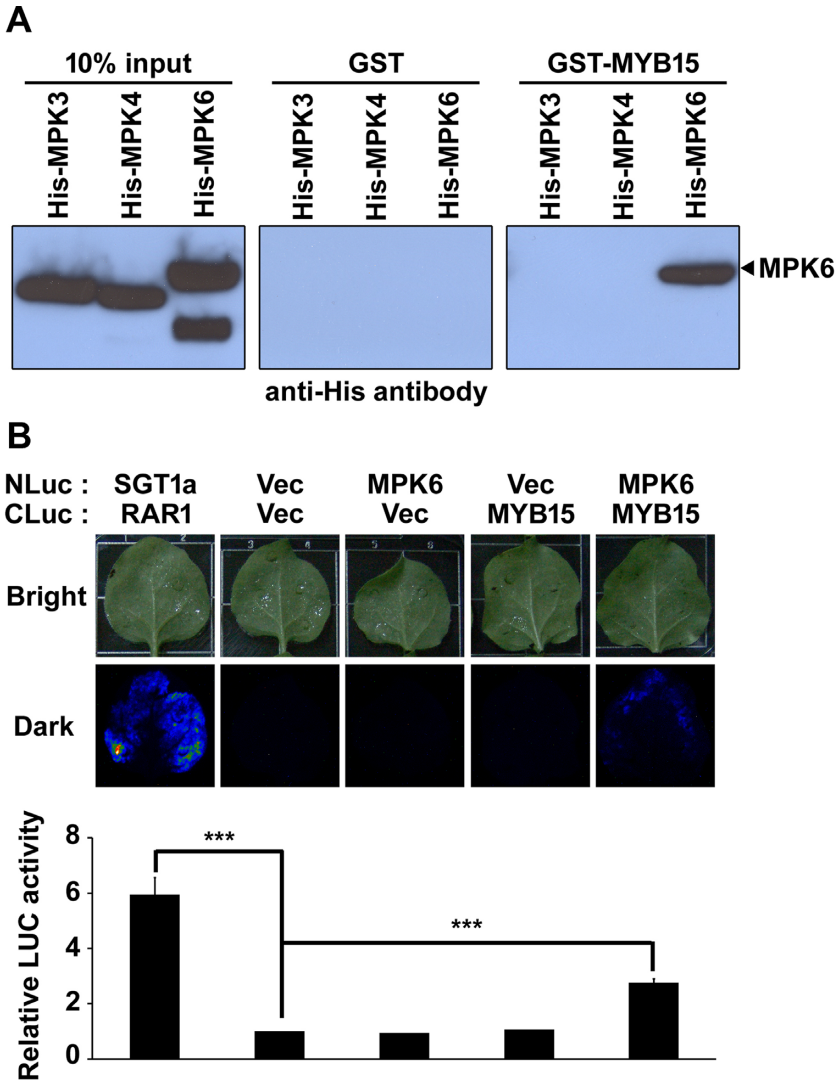

Figure 1. MYB15 interacts with MPK6 *in vitro* and *in planta*. (**A**) Pull-down assay demonstrating the specificity of the interaction of MPK with MYB15. Shown is chemiluminescence detection of $(His)_6$ on blots of SDS-polyacrylamide gels loaded with (left to right panels) input His-MPKs, GST and GST-MYB15 pull-down proteins. (**B**) LUC complementation imaging assay to detect the interaction of MPK6 with MYB15 in *Nicotiana benthamiana* leaves. Shown in the upper panel are images and luminescence of *N. benthamiana* leaves co-infiltrated with *Agrobacterium* strains containing the indicated combinations of NLuc- and CLuc-fusion constructs. The SGT1a-NLuc/CLuc-RAR1 combination was used as a positive control. Vec refers to NLuc and CLuc empty vectors. Leaves were photographed at 3 days after infiltration. Shown in the lower panel is the quantification of LUC activity in these leaves. The luminescence intensities are expressed relative to that of leaves infiltrated with the NLuc Vec/CLuc Vec combination. Data are presented as the mean ± SD of three independent experiments. $P < 0.001$ (***) indicate statistically significant changes.

freezing bath set at 0°C. For each temperature treatment, three replicates were performed. The temperature of the bath was programmed to decrease to −10°C at a rate of 2°C per h. When the designated temperature was reached, the tubes were removed and placed immediately on ice to allow gradual thawing. The leaflets then were transferred carefully to another tube containing 20 ml of deionized water and shaken overnight, followed by conductivity measurements. The tubes containing leaves were then autoclaved. After cooling to room temperature for 4 h, the conductivity of the solution was again measured. The percentage of electrolyte leakage was calculated as the percentage of conductivity before autoclaving over that after autoclaving.

Plant freezing assay

Freezing stress was applied to 3-week-old plants grown in soil at 22°C under a long-day photoperiod by exposing them sequentially to 4°C for 1 h, followed by 0°C for 1 h and a programmed cycle of temperature reduction at a rate of 1°C per h to −8°C. After the freezing treatment, the plants were incubated at 4°C for 1 day, followed by a return to 22°C. Survival was evaluated 5 days later.

RESULTS

MYB15 interacts with MPK6

Separate high-throughput analyses initially identified MYB15 as a putative substrate for activated MPK6 and

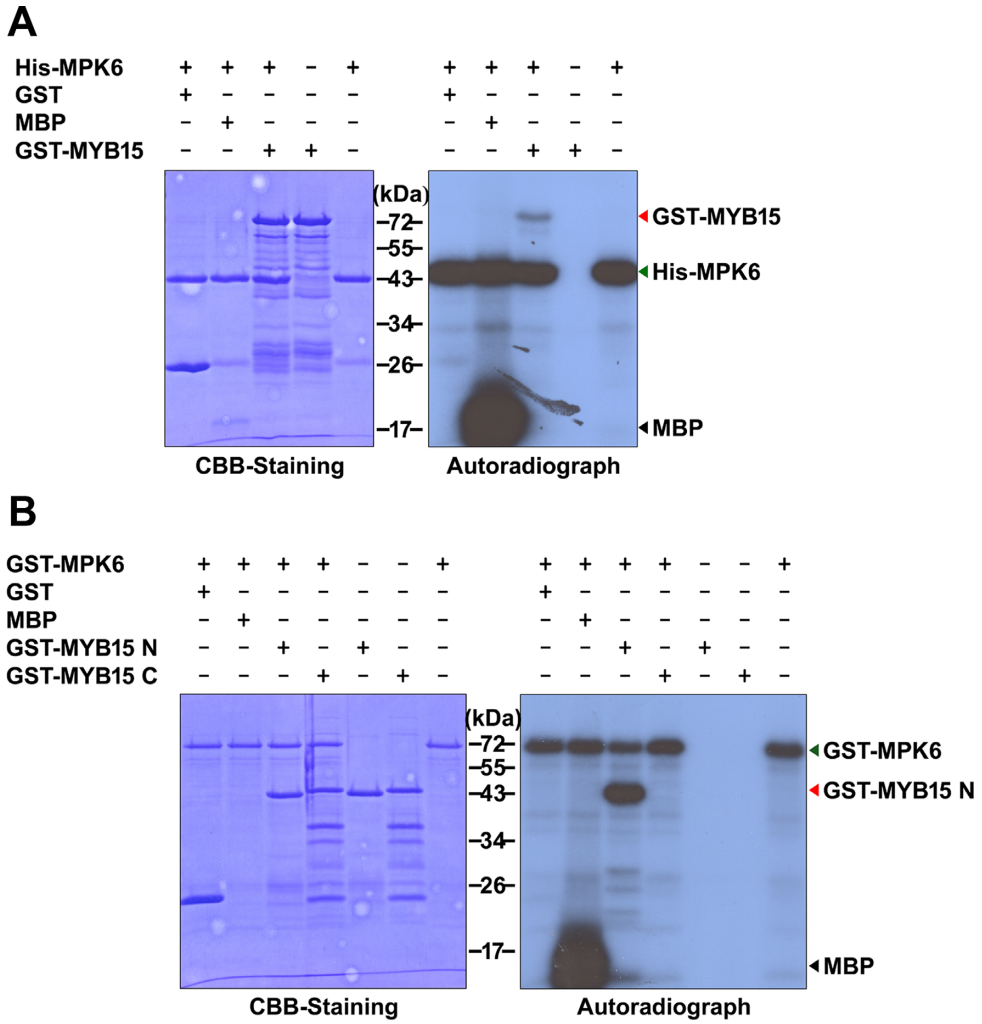

Figure 2. *In vitro* phosphorylation of MYB15 by recombinant MPK6. Coomassie Brilliant Blue (CBB) staining (**A**) and autoradiography (**B**) of an SDS-polyacrylamide gel with resolved kinase reactions containing the indicated combinations of purified *Escherichia coli*-expressed proteins and [γ-^{32}P] ATP. Abbreviations: MBP, myelin basic protein; GST-MYB15, GST-tagged full-length MYB15; GST-MYB15N, GST-tagged MYB15 N-terminal fragment (amino acids 1–172) and GST-MYB15C, GST-tagged MYB15 C-terminal fragment (amino acids 173–285). MBP and GST were used as positive and negative control substrates, respectively.

as an MPK6-interacting protein (4,20,22). Therefore, we re-examined the interaction between MYB15 and MPK6 using yeast two-hybrid analysis. As shown in Supplementary Figure S1, yeast cells co-expressing MYB15 and MPK6 grew on selective medium lacking adenine and acquired β-galactosidase activity, indicating a positive interaction between these proteins.

We then examined the specificity of the interaction of MYB15 with *Arabidopsis* MPKs using a pull-down assay (Figure 1A). As shown on the immunoblots, approximately equal amounts of the three MPKs were loaded onto the beads (left panel) and no His-MPKs were detected in eluates of immobilized GST-beads (middle panel). However, His-MPK6, but not His-MPK3 or His-MPK4, was detected in the eluates of immobilized GST-MYB15-beads (right panel). These results indicate that MYB15 interacts directly and specifically with MPK6 *in vitro*.

We examined the interaction of MYB15 with MPK6 *in planta* in *N. benthamiana* leaves using an LUC complementation imaging assay. As shown in Figure 1B, strong LUC activity was detected at 3 days post-inoculation in positive control leaves co-infiltrated with *Agrobacterium* strains carrying *CaMV35S*: *SGT1a-NLuc* and *CaMV35S*: *CLuc-RAR1* (26). No LUC activity was detected in leaves co-infiltrated with *Agrobacterium* strains carrying *CLuc* vector plus *NLuc* vector, *CaMV35S*: *MPK6-NLuc* plus *CLuc* vector or *CaMV35S*: *CLuc-MYB15* plus *NLuc* vector combinations. However, LUC activity was detected in leaves co-infiltrated with *Agrobacterium* strains carrying *CaMV35S*: *MPK6-NLuc* plus *CaMV35S*: *CLuc-MYB15* at levels ∼2- to 3-fold higher than that of control leaves co-infiltrated with empty vector(s). These results suggest that MYB15 directly interacts with MPK6 *in planta*.

MYB15 is phosphorylated by recombinant MPK6

Having confirmed that MYB15 interacts directly with MPK6, we examined the ability of MPK6 to phosphorylate MYB15 using an *in vitro* kinase assay with *E. coli*-expressed

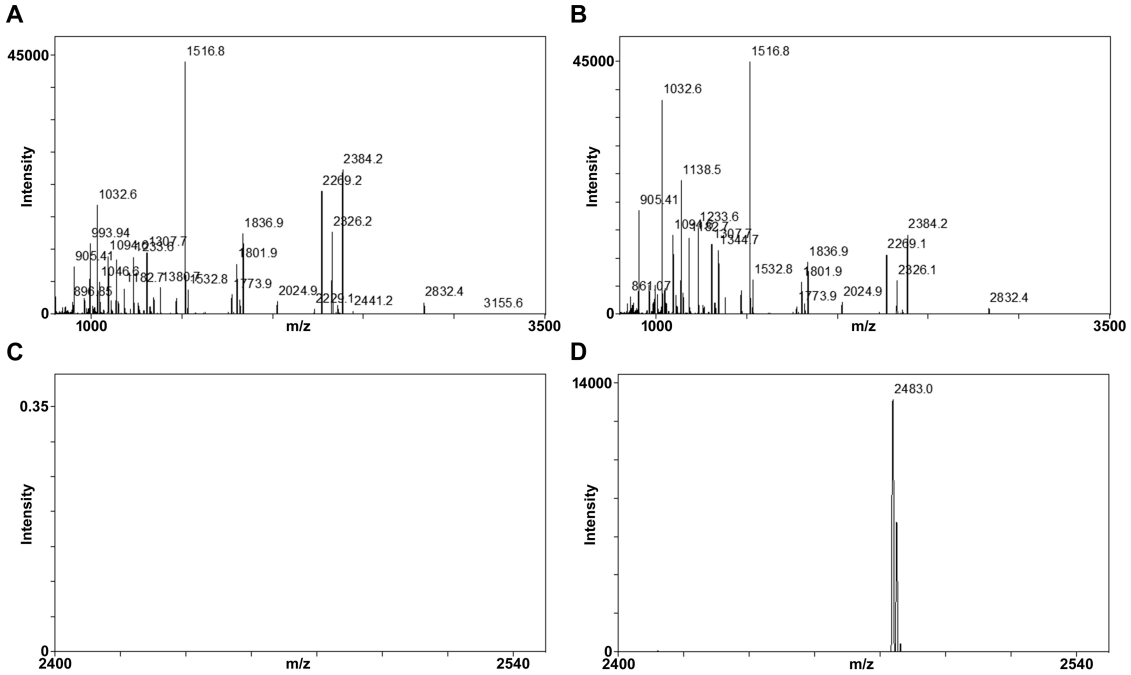

Figure 3. Identification of MPK6-phosphorylated peptides in GST-MYB15N using TiO_2 chromatography and MALDI-TOF mass spectrometry. (**A** and **B**) Shown are the peptide mass fingerprint of unphosphorylated (A) or MPK6-phosphorylated (B) GST-MYB15 N-terminal fragment (amino acids 1–172) after trypsin digestion and without TiO_2 purification. A database search of mass data identified GST and MYB15N in the sample with 62 and 38% coverage, respectively. (**C** and **D**) Shown are the mass fingerprints of phosphopeptides recovered after TiO_2 enrichment from tryptic digests of unphosphorylated (C) or MPK6-phosphorylated (D) GST-MYB15N. One phosphopeptide peak (m/z 2482.9) originating from SESELADSSNPSGESLFSTSPSTS was detected from phosphorylated GST-MYB15N (D) but not from unphosphorylated GST-MYB15N (C).

purified proteins and [γ-^{32}P] ATP. After separating the proteins by SDS-PAGE, we detected the phosphorylated proteins on the gel by autoradiography and visualized total proteins with CBB staining. As shown in Figure 2A, an autophosphorylation band of ∼48 kDa corresponding to His-MPK6 was observed in all samples. No phosphorylation band was observed corresponding to GST (∼25 kDa), the negative control substrate, whereas MBP (∼18.5 kDa; positive control) and GST-MYB15 (∼72 kDa) were phosphorylated by MPK6. Since MPKs usually phosphorylate Ser and Thr residues on S/T-P motifs, two MPK phosphorylation sites can be predicted in MYB15, on Thr18 and Ser168. To verify this prediction, we performed an *in vitro* kinase assay using purified GST-tagged MYB15 N-terminal fragment (GST- GST-MYB15N; amino acids 1–172, ∼45 kDa) and GST-tagged MYB15 C-terminal fragment (GST-MYB15C; amino acids 173–285, ∼45 kDa) as substrates for GST-MPK6 (∼72 kDa). GST-MPK6 autophosphorylation bands were detected in all samples (Figure 2B). A phosphorylation band was observed when we used GST-MYB15N as the substrate, but not with GST-MYB15C, suggesting that MYB15 is phosphorylated by MPK6 at the predicted sites.

Identification of a phosphorylation site in MYB15 by mass spectrometry

We investigated the MPK6-phosphorylation sites in MYB15 by mass spectrometry analysis after selectively enriching for phosphopeptides by TiO_2 chromatography (Figure 3). A kinase reaction was performed with purified GST-MYB15N in the presence and absence of purified His-MPK6. After SDS-PAGE, we excised the bands corresponding to GST-MYB15N, digested them with trypsin and subjected the resulting peptides to MALDI-TOF MS. The mass spectrum of the phosphorylated sample prior to TiO_2 chromatography identified the protein as GST and MYB15 with 56 and 34% coverage, respectively (Figure 3B). After TiO_2 chromatography, one phosphopeptide was identified, as shown in Figure 3D and Supplementary Table S4. MPKs usually phosphorylate their substrates on Ser or Thr residues that are followed by a proline (Pro, P) (S/T-P motif). The phosphopeptide that was identified contained one putative MPK6 phosphorylation site, Ser168 (SESELADSSNPSGESLFSTS$_{168}$PSTS). Therefore, Ser168 of MYB15 was identified as a putative MPK6 phosphorylation site.

To confirm the phosphorylation site of MYB15, we performed *in vitro* kinase assays using point mutants of MYB15 as substrates. Specifically, purified GST-MYB15, GST-MYB15^{T18A}, GST-MYB15^{S168A} and GST-MYB15$^{T18A/S168A}$ (GST-MTB15^{AA}) were used as substrates for His-MPK6. As shown in Figure 4, the intensity of the radiolabeled His-MPK6 band, indicating autophosphorylation, was roughly equal in all samples, confirming the presence of sufficient enzyme activity in all samples. Radiolabeled proteins of the expected size of GST-MYB15 (∼72 kDa) were detected in samples containing His-MPK6 along with GST-MYB15 or GST-MYB15^{T18A}, indicating their phosphorylation. However, phosphorylation of GST-MYB15^{S168A} and GST-MTB15^{AA} by His-MPK6 al-

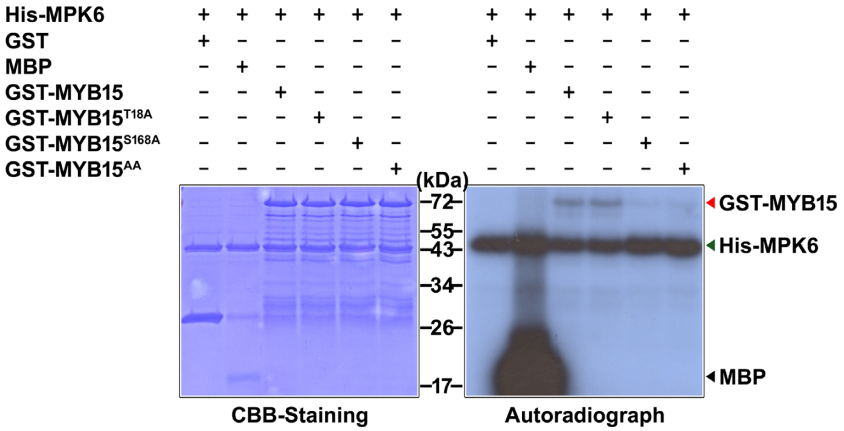

Figure 4. Identification of MPK6-phosphorylation sites on MYB15 by site-directed mutagenesis. Coomassie Brilliant Blue (CBB) staining and autoradiography of an SDS-polyacrylamide gel with resolved kinase reactions containing the indicated combinations of purified *Escherichia coli*-expressed proteins and [γ-^{32}P] ATP. The mutant full-length MYB15 proteins MYB15^{T18A}, MYB15^{S168A} and MYB15$^{T18A/S168A}$ (MYB15^{AA}) were generated by site-directed mutagenesis. Myelin basic protein (MBP) and GST were used as positive and negative controls, respectively.

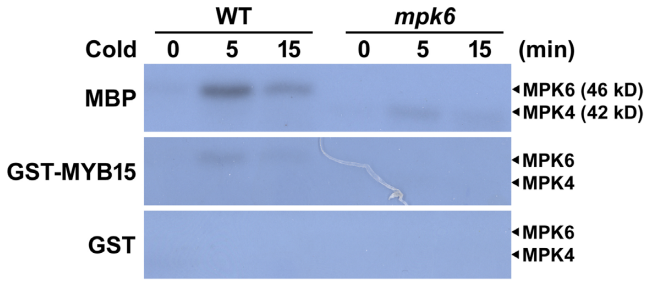

Figure 5. MYB15 is phosphorylated by cold-activated plant MPK6. Leaves of 3-week-old wild-type (WT) and *mpk6* plants were subjected to cold (4°C) treatments for the indicated times to induce MPK activity. Shown are autoradiographs of SDS-polyacrylamide gels containing embedded MBP, GST-MYB15 and GST, depicting signals from an in-gel kinase assay on resolved proteins from extracts of treated leaves. The expected positions of MPK4 and MPK6 on the gels are indicated.

most disappeared compared to that seen in MYB15 or MYB15^{T18A} proteins, even though faint bands were detected. Since mass spectrometry failed to identify any specific phosphorylation sites other than Ser168, these faint bands may indicate that the mutant proteins MYB15^{S168A} and MTB15^{AA} are non-specifically phosphorylated by MPK6 because of high protein levels in the assays (Figure 3). Thus, Ser168 residue is necessary and sufficient for MPK6-induced phosphorylation of MYB15.

MYB15 is phosphorylated by cold-activated plant MPK6

Immunocomplex kinase assays showed that cold stress activates endogenous MPK4 and MPK6 (4). To confirm that endogenous MPKs are activated by cold stress, we performed an in-gel kinase assay using MBP as substrate in cold stress-treated WT, *mpk3* and *mpk6* seedlings. MPK6 was mainly activated by cold stress (Supplementary Figure S2). To determine whether MYB15 is phosphorylated by native MPK6 and to associate MPK6-MYB15 signaling with cold stress, we performed an in-gel kinase assay using purified GST-MYB15, GST (negative control) and MBP (positive control) embedded in the gels and fractionated cell-free extracts prepared from 3-week-old WT and *mpk6* seedlings subjected to cold stress for various time periods (Figure 5). No radiolabeled bands were detected in extracts from unstressed (0 min) WT, or *mpk6* mutant leaves in gels embedded with GST-MYB15 (Figure 5). A radiolabeled phospho-MYB15 band at the expected location of MPK6 (∼46 kDa) was detected in the GST-MYB15-embedded gel containing resolved extracts of WT leaves, but not in the gel containing resolved extracts of *mpk6* leaves from cold stress-treated plants. The phosphorylation of MYB15 was rapid and transient, as is expected if the phosphorylation requires activated endogenous MPK6. A similar pattern of phosphorylation was observed in the gel embedded with MBP, and no bands were observed in the gel embedded with GST (Figure 5). These observations suggest that MYB15 can be phosphorylated by native MPK6 and that the MPK6-MYB15 pathway participates in cold stress signaling.

MPK6-induced phosphorylation of MYB15 affects its DNA-binding affinity

MYB15 binds to the promoters of *CBFs* and represses their transcription (23). Therefore, we hypothesized that the binding affinity of MYB15 to *CBF* promoters is regulated by MPK6-phosphorylation of MYB15. We tested this hypothesis by performing electrophoretic mobility shift assays (EMSAs) using purified proteins expressed in *E. coli*, with a radiolabeled *CBF3* promoter fragment (−984 to −785 bp region) as a probe. This *CBF3* promoter fragment binds strongly to MYB15 and contains two MYB recognition sequences (23). As expected (Figure 6), a shifted band was observed when the probe was incubated with GST-MYB15, but not with GST alone. The intensity of this shifted band decreased when a competitive unlabeled probe was added in a concentration-dependent manner (Supplementary Figure S3), indicating that MYB15 specifically interacts with MYB recognition sequences. No shifted band was detected when GST-MYB15 was incubated with His-MPK6 and ATP prior to the addition of the probe, suggesting that the phosphorylation of MYB15 by MPK6 diminishes its binding affinity (Figure 6A). The shifted band was observed with

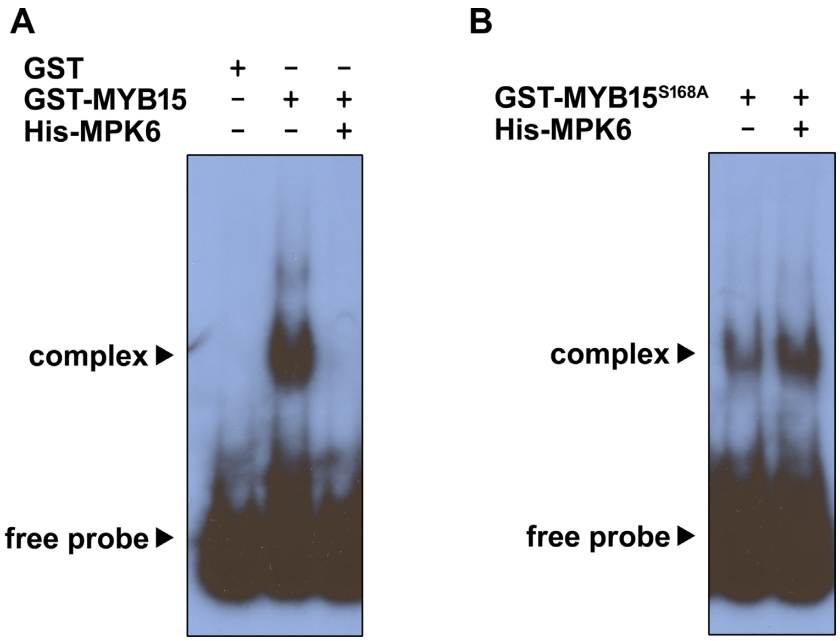

Figure 6. Binding affinity of MYB15 to the *CBF3* promoter fragment is reduced by MPK6-induced phosphorylation. Shown are the results of an EMSA performed using a ^{32}P-labeled *CBF3* promoter fragment (−984 to −785 bp region) as a probe. Equal amounts of purified *Escherichia coli*-expressed GST, GST-MYB15 (**A**) and GST-MYB15^{S168A} (**B**) were incubated in the absence or presence of purified His-MPK6 at 30°C for 30 min before adding the probe.

GST-MYB15^{S168A} and when GST-MYB15^{S168A} was pre-incubated with His-MPK6 and ATP (Figure 6B), suggesting that the loss of binding ability is mediated by phosphorylation of MYB15 by MPK6 at Ser168.

Phosphorylation of MYB15 is necessary for derepression of *CBF3* gene expression

To investigate whether the transcriptional activity of MYB15 is regulated by its phosphorylation, we performed transient expression assays with *Arabidopsis* protoplasts (Figure 7) using the effector plasmids and reporter plasmids shown in Figure 7A. The relative GUS activity level was reduced (50.75 ± 2.84%) in protoplasts co-transfected with *CaMV35S: MYB15* and reporter plasmid compared with protoplasts co-transfected with effector vector and reporter plasmid (100%); this was expected because MYB15 functions as a transcriptional repressor (Figure 7B). Interestingly, relative GUS activity was even lower (31.17 ± 6.55%) in protoplasts co-transfected with *CaMV35S: MYB15^{S168A}* and reporter plasmid (Figure 7B). Protoplasts are more sensitive to subtle external stresses compared with normal plant cells; therefore, even in the absence of applied stress, MPKs can be somewhat activated in protoplasts (38). In fact, the activity of MPK6 extracted from protoplasts was increased compared with that of MPK6 from plant seedlings (0 min) (Supplementary Figure S4). Therefore, GUS activity was partly recovered in protoplasts transfected with MYB15 because some MYB15 proteins were phosphorylated by MPK6 and released from the promoter. In contrast, MYB15^{S168A} proteins are unresponsive to MPK6 and are not released from the promoter at all. These results support that transcriptional activation of *CBF3* is positively regulated by MPK6-induced phosphorylation of MYB15 at Ser168.

Phosphorylation of MYB15 is required for the upregulation of *CBF* genes

To examine the importance of an intact MPK6-phosphorylation site for the regulation of *CBF* genes and freezing tolerance by MYB15, we generated transgenic *CaMV35S:3XFlag-MYB15* (MYB15 OX) and *CaMV35S:3XFlag-MYB15^{S168A}* (MYB15^{S168A} OX) lines via *Agrobacterium*-mediated transformation. We selected three independent MYB15 OX and MYB15^{S168A} OX lines based on high levels of MYB15 expression (Supplementary Figure S5). We investigated the expression of *CBF* in each of these three lines subjected to cold stress for 3 h. Transcription of *CBF* decreased when MYB15 was overexpressed, and even more so when MYB15^{S168A} was expressed (Supplementary Figure S6). Each of these three independent lines showed similar expression patterns and *CBF* levels. Therefore, we mixed seeds from these lines together and used these for further studies.

First, we compared the expression levels of *CBF* genes in seedlings harboring empty vector, MYB15 OX and MYB15^{S168A} OX subjected to cold stress for various time periods (Figure 8). As expected (Agarwal *et al.*, (23), the levels of *CBF1, CBF2* and *CBF3* transcripts increased upon cold treatment in all lines. The accumulation of all *CBF* transcripts peaked at 2 h of treatment in empty vector control and MYB15 OX plants but at 4 h in MYB15^{S168A} OX. At 2 h of treatment, the transcript levels of *CBF1, CBF2* and *CBF3* were significantly lower in MYB15 OX seedlings than in the empty vector control and were lowest in MYB15^{S168A}

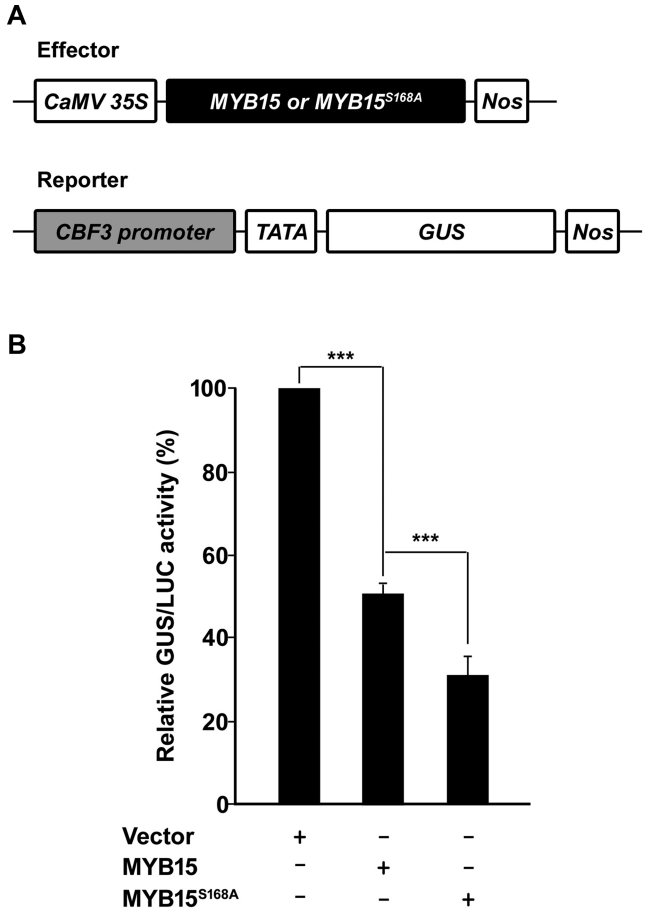

Figure 7. Transcriptional repression activity of MYB15 is enhanced by a mutation in its phosphorylation site. (**A**) Schematic representation of reporter and effector constructs used in the transient expression assay. The effector construct consisted of the *CaMV35S* promoter fused to the full-length *MYB15* and *MYB15*^{S168A} ORFs. The *CBF3* promoter (−2000 to −1 bp region) was fused to the *GUS* reporter gene containing a minimal *CaMV35S* promoter to generate the reporter construct. (**B**) Transient assay of *CBF3* expression in *Arabidopsis* protoplasts. The GUS//LUC activities of *Arabidopsis* protoplasts that were co-transfected with the *CBF3*:*GUS* reporter plasmid, a *CaMV35S*:*LUC* internal control plasmid and the indicated effector plasmids were measured. Shown are relative GUS/LUC activities, which were calculated as a percentage of the GUS/LUC activities of samples transformed with the reporter construct plus empty effector vector. Data are presented as the mean ± SD of three independent experiments. $P < 0.001$ (***) indicate statistically significant changes.

OX. The differences became less pronounced with increasing duration of cold treatment.

We then conducted an ion leakage test to evaluate the effect of MYB15 phosphorylation on freezing tolerance. Overexpression of MYB15 increased ion leakage in non-acclimated plants compared to the control, as previously reported (23), indicating increased freezing sensitivity (Figure 9A). The LT_{50} (the temperature of 50% ion leakage) values for empty vector control and MYB15 OX plants were −6.7°C and −5.7°C, respectively. The LT_{50} value for MYB15^{S168A} OX plants was −5.4°C, that is, lower than that of MYB15 OX plants, indicating that these plants had the greatest freezing sensitivity among the lines tested. We also evaluated the role of MYB15 phosphorylation by performing a whole-plant freezing-survival test on 3-week-old soil-grown plants. As shown in Figure 9B and 9C, the lowest amount of tissue death was observed in leaves of empty-vector control plants and MYB15 OX plants were more sensitive to freezing than empty-vector plants but more tolerant than MYB15^{S168A} OX plants. Therefore, the loss of the MPK6-phosphorylation site on MYB15 is associated with reduced freezing tolerance.

DISCUSSION

MPK6 phosphorylates MYB15

MPK cascades are universal and highly conserved signal transduction modules that are present in all eukaryotes, including plants (10,39). These protein phosphorylation cascades link extracellular stimuli to a wide range of cellular responses. However, to date, only a limited number of MPK substrates have been found in plants. In this study, we provide experimental evidence that MYB15 is a substrate of MPK6. First, MYB15 specifically and directly interacted with MPK6 *in vitro* and *in planta*. Second, MYB15 was phosphorylated by recombinant MPK6 and cold-activated plant MPK6, as revealed by *in vitro* and *in-gel* kinase assays, respectively. Third, the site of MYB15 phosphorylation by MPK6 was identified by mass spectrometry and confirmed by site-directed mutagenesis. MYB15 is a member of the R2R3 family of MYB transcription factors, which control plant development, secondary metabolite biosynthesis and responses to environmental stresses (40,41). The activities of plant MYBs are regulated by phosphorylation. For example, NtMYBA2 is activated by the phosphorylation of a cyclin–CDK complex through the repression of its inhibitory domain (42,43). The DNA-binding ability of MYB41 is enhanced by the phosphorylation of MPK6, which is required for its physiological function in salt-stress tolerance (44). The phosphorylation of MYB44 by MPK3/MPK6 is required for the inhibition of seed germination (45). Also, phosphorylation is required for the activity of ZAT10, a positive regulator of osmotic stress tolerance in *Arabidopsis* (46). In addition, high-throughput protein microarray analysis in *Arabidopsis* revealed that many MYB proteins are potential targets of MPKs (20). In animal cells, murine c-Myb is phosphorylated and regulated by another MPK, p42^{mpk} (47). The activity of B-Myb is also altered by the phosphorylation of the cyclin-dependent kinase (CDK) complex (48–51). Thus, the phosphorylation of MYB proteins by protein kinases appears to be an evolutionarily conserved regulatory mechanism.

The MPK cascade triggered by cold stress comprises MEKK1, MKK2, MPK4 and MPK6. Although MPK4 and MPK6 are activated by cold stress downstream of MEKK1–MKK2, we did not find experimental evidence for the direct regulation of MYB15 by MPK4, suggesting that MYB15 may not be a target of MPK4 during cold stress signaling. Therefore, MPK4 may be involved in cold stress signaling through a different pathway or a different substrate, which remains to be investigated.

DNA binding of MYB15 is reduced by its phosphorylation

The transcript and protein levels of plant MYB transcription factors are regulated by microRNAs and ubiquitin-

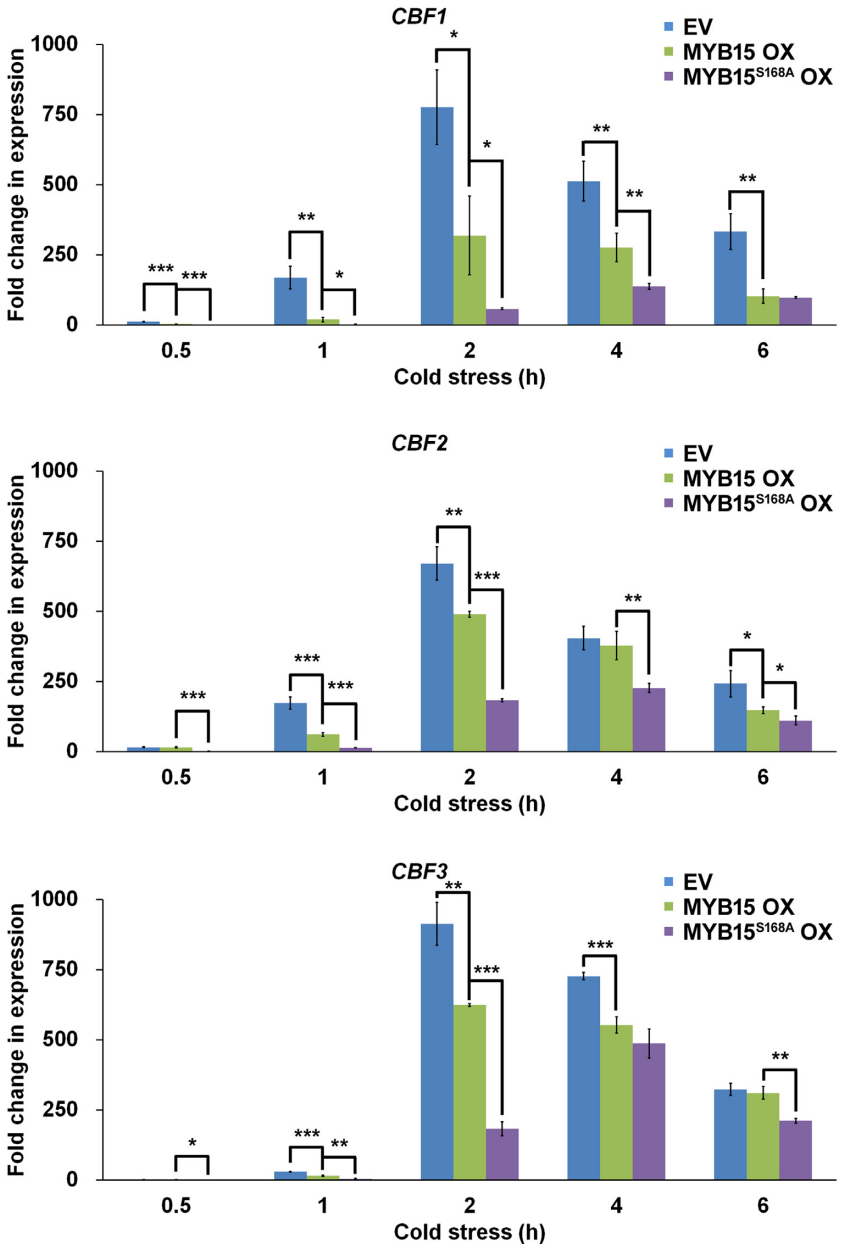

Figure 8. Mutation of the MYB15 phosphorylation site increases its transcriptional repression of *CBF* genes in cold-stressed transgenic plants. *CBF* expression was measured in transgenic plants expressing empty vector (EV), MYB15 and MYB15^{S168A} under cold stress. Quantitative RT-PCR analysis of *CBF* genes was performed using total RNA isolated from seedlings of the indicated lines subjected to cold (4°C) treatment for the indicated times. The cDNA was synthesized from 5 μg of total RNA and used as a template for RT-PCR. Data are presented as the mean ± SD of three independent experiments. $P < 0.05$ (*), $P < 0.01$ (**) and $P < 0.001$ (***) indicate statistically significant changes.

mediated degradation, respectively (52). The activities of plant MYB proteins are thought to be governed by protein–protein interactions, redox control and phosphorylation. The phosphorylation of transcription factors can alter their subcellular location, stability, DNA-binding affinity and interactions with other regulatory proteins (53). As shown in Figures 6–8, the phosphorylation of MYB15 reduces its DNA-binding affinity to the promoters of *CBF* genes. In addition, a mutation in its phosphorylation site, MYB15^{S168A}, disrupted its dissociation from the *CBF3* promoter and the induction of cold-responsive genes such as *CBF1*, *CBF2* and *CBF3*. Similarly, the binding of *Am*MYB340 to target DNA is inhibited by phosphorylation in *Antirrhinum majus* (54). Conversely, the transcriptional activities of PtMYB4 and AtMYB46 are positively regulated by phosphorylation in *Pinus taeda* and *Arabidopsis thaliana*, respectively (55). Ser168, the phosphorylation site of MYB15, is distantly located from an R2R3 DNA-binding domain corresponding to 11–116 amino acid residues. Therefore, it is unlikely that MYB15 phosphorylation directly changes the DNA binding ability of the R2R3 DNA-binding domain. Instead, it is more likely that the phosphoryla-

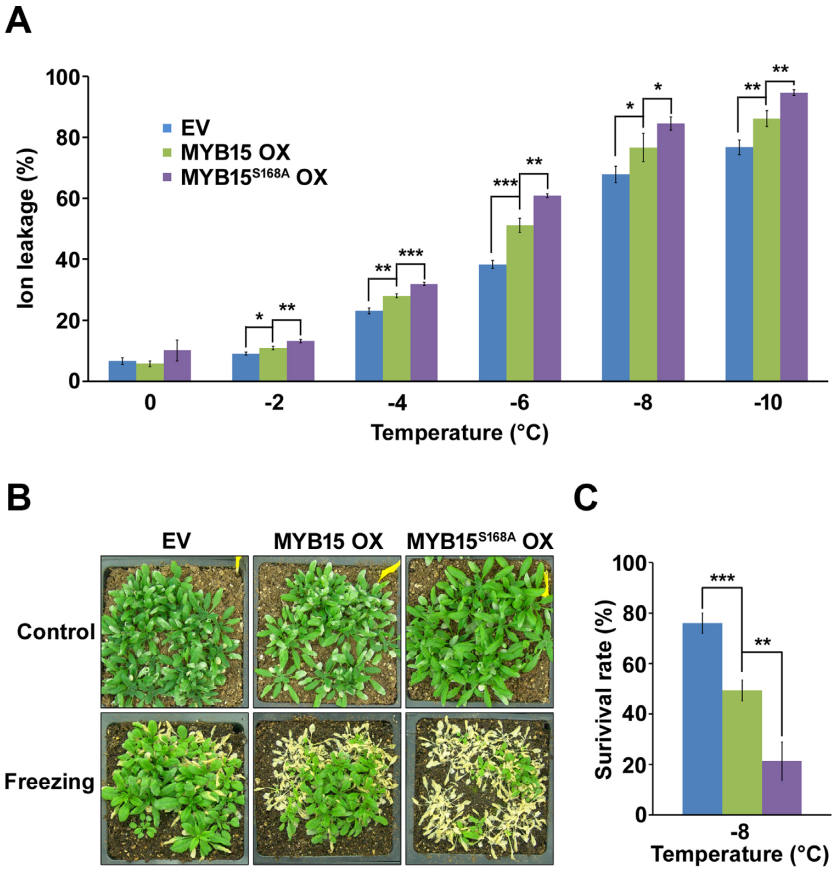

Figure 9. Freezing tolerance is reduced by a mutation of MYB15 that prevents phosphorylation. (**A**) Ion-leakage test without cold acclimation. Empty vector (EV), MYB15 OX and MYB15^{S168A} OX transgenic plants were used. The ion leakage experiment was repeated twice with three replicates per experiment. Shown are results from one representative experiment. Data are presented as the mean ± SD of three independent experiments. $P < 0.05$ (*), $P < 0.01$ (**) and $P < 0.001$ (***) indicate statistically significant changes. (**B** and **C**) Freezing survival assay without acclimation. Three-week-old plants grown in soil at 22°C were incubated at 4°C for 1 h, followed by freezing treatment for 2 h at −8°C. After the freezing treatment, plants were incubated at 4°C for 1 day and returned to normal growing conditions for 5 days before photography (B) and survival rate measurements (C). Data are presented as the mean ± SD of three independent experiments. $P < 0.01$ (**) and $P < 0.001$ (***) indicate statistically significant changes.

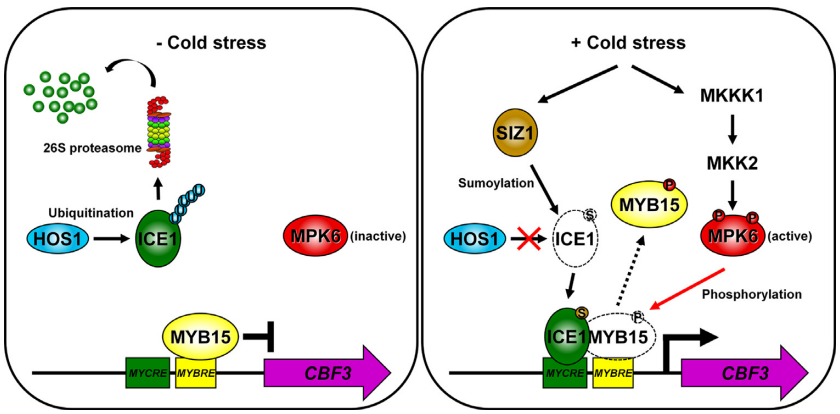

Figure 10. Model of the role of MYB15 in cold stress signaling. Under normal conditions, ICE1 is ubiquitinated by HOS1 and degraded by the 26S-proteasome pathway, whereas MYB15 binds to an *MYBRE* on the promoters of *CBF* genes to inhibit their transcription. In response to cold stress, MYB15 is phosphorylated by cold-activated MPK6 and released from the *CBF* gene promoters. ICE1 is stabilized by SIZ1-mediated sumoylation and sumoylated ICE1 binds to an MYCRE on the *CBF* promoters, leading to their increased expression and increased freezing tolerance. *CBFs*, C-repeat binding factors (an AP2-type transcription factors); *MYBRE*, MYB transcription factor recognition element; *MYCRE*, MYC transcription factor recognition element; P, phosphorylation; S, sumoylation; U, ubiquitination.

tion of MYB15 by MPKs is necessary for its conformational change, which induces its release from the promoters of cold-responsive genes. It is also possible that changes in hydrogen bonding capacity and electrostatic interactions caused by MYB15 phosphorylation affect the binding affinity between MYB15 and DNA. Therefore, structural comparisons of non-phosphorylated versus phosphorylated MYB15 would help clarify the molecular mechanism by which protein phosphorylation modulates MYB15 DNA-binding affinity.

Phosphorylation of MYB15 by MPK is required for freezing tolerance

Cold-mediated signaling during the freezing tolerance response requires fine-tuned transcriptional regulation. Cold temperatures trigger the transcription of *CBF* genes encoding transcription factors, which in turn activate the transcription of genes containing the DRE/CRT promoter element (1,56). The transcription of *CBF* genes is tightly controlled; uncontrolled expression of *CBF* genes may adversely affect growth and development (34,57,58). *CBF* genes are positively and negatively regulated by the transcription factors ICE and MYB15, respectively. ICE1 is a MYC-like bHLH transcription factor that binds to MYC elements of *CBF* gene promoters and activates their expression (3). Under normal conditions, ICE1 is ubiquitinated by the E3 ligase HOS1 and degraded by the 26S-proteasome pathway, whereas under cold conditions, ICE1 is stabilized by SIZ1-mediated sumoylation (59,60). MYB15 binds to MYB elements in the promoters of *CBFs* and negatively regulates their expression (23). However, the way(s) in which bound MYB15 is released from *CBF* promoters in response to cold stress has not yet been investigated.

In the current study, we demonstrated that the DNA-binding ability of MYB15 is reduced by the phosphorylation activity of a cold-responsive MPK, releasing its repression of gene transcription. In our proposed model (Figure 10), under normal conditions, *CBF* transcription is repressed by the DNA-binding of unphosphorylated MYB15 to MYB recognition elements in their promoters and the absence of ICE1 activity. In response to cold stress, MYB15 is phosphorylated by cold-activated MPK6. The phosphorylated MYB15 dissociates from *CBF* promoters because of its reduced DNA-binding affinity. ICE1 that has been stabilized by SIZ1-mediated sumoylation binds to the MYC recognition elements in the *CBF* promoters and activates the expression of *CBF* genes, thereby conferring freezing tolerance to the plant. This suggests that release of MYB15 from the promoter is required for the activation of ICE1-mediated *CBF* genes because overexpression of $MYB15^{S168A}$ inhibits cold activation of *CBF* (Figure 8). It also suggests that $MYB15^{S168A}$ binds DNA in the presence of activated MPK6 (Figure 6B). To further elucidate the transcriptional regulation of *CBF* genes during the cold response, however, detailed studies should be performed on the release of MYB15 and the binding of ICE1 to the promoters of these genes.

SUPPLEMENTARY DATA

Supplementary Data are available at NAR Online.

ACKNOWLEDGEMENTS

We thank Dr Dae-Jin Yun for critical comments of the article, and Dr Yong-Hwan Moon for helpful discussions and critique of the article.

Author contributions: S.H.K. and W.S.C. designed, planned and organized the experiments. S.H.K., S.B., and J.A. generated all *Arabidopsis* transgenic lines and all plant materials used in this study. S.H.K., H.S.K., S.B., J.A. and Y.Y. performed the research. S.H.K., J.Y.K. and W.S.C. analyzed the data. S.H.K. and W.S.C. wrote the article.

FUNDING

Next-Generation BioGreen 21 Program by the Rural Development Administration [#PJ01109101]; Basic Science Research Program through the National Research Foundation of Korea (NRF) by the Ministry of Education [2015R1D1A4A01020200]; National Research Foundation of Korea (NRF) grant by the Korean government (MSIP) [2016R1A2B4015859]. Funding for open access charge: Next-Generation BioGreen 21 Program by the Rural Development Administration [#PJ01109101].

Conflict of interest statement. None declared.

REFERENCES

1. Thomashow,M.F. (1999) PLANT COLD ACCLIMATION: freezing tolerance genes and regulatory mechanisms. *Annu. Rev. Plant Physiol. Plant Mol. Biol.* **50**, 571–599.
2. Shinozaki,K., Yamaguchi-Shinozaki,K. and Seki,M. (2003) Regulatory network of gene expression in the drought and cold stress responses. *Curr. Opin. Plant Biol.* **6**, 410–417.
3. Chinnusamy,V., Ohta,M., Kanrar,S., Lee,B.H., Hong,X., Agarwal,M. and Zhu,J.K. (2003) ICE1: a regulator of cold-induced transcriptome and freezing tolerance in Arabidopsis. *Genes Dev.* **17**, 1043–1054.
4. Teige,M., Scheikl,E., Eulgem,T., Doczi,R., Ichimura,K., Shinozaki,K., Dangl,J.L. and Hirt,H. (2004) The MKK2 pathway mediates cold and salt stress signaling in *Arabidopsis*. *Mol. Cell***15**, 141–152.
5. Stockinger,E.J., Gilmour,S.J. and Thomashow,M.F. (1997) *Arabidopsis thaliana CBF1* encodes an AP2 domain-containing transcriptional activator that binds to the C-repeat/DRE, a cis-acting DNA regulatory element that stimulates transcription in response to low temperature and water deficit. *Proc. Natl. Acad. Sci. U.S.A.* **94**, 1035–1040.
6. Liu,Q., Sakuma,Y., Abe,H., Kasuga,M., Miura,S., Yamaguchi-Shinozaki,K. and Shinozaki,K. (1998) Two transcription factors, DREB1 and DREB2, with an EREBP/AP2 DNA binding domain separate two cellular signal transduction pathways in drought- and low-temperature-responsive gene expression, respectively, in Arabidopsis. *Plant Cell* **10**, 1391–1140.
7. Zhang,S. and Klessig,D.F. (2001) MAPK cascades in plant defense signaling. *Trends Plant Sci.* **6**, 520–527.
8. Jonak,C., Ökrész,L., Bögre,L. and Hirt,H. (2002) Complexity, crosstalk and integration of plant MAP kinase signalling. *Curr. Opin. Plant Biol.* **5**, 415–424.
9. Tena,G., Boudsocq,M. and Sheen,J. (2011) Protein kinase signaling networks in plant innate immunity. *Curr. Opin. Plant Biol.* **14**, 519–529.
10. Colcombet,J. and Hirt,H. (2008) *Arabidopsis* MAPKs: a complex signalling network involved in multiple biological processes. *Biochem. J.*, **413**, 217–226.
11. Group,MAPK (2002) Mitogen-activated protein kinase cascades in plants: a new nomenclature. *Trends Plant Sci.*, **7**, 301–308.
12. Ichimura,K., Mizoguchi,T., Yoshida,R., Yuasa,T. and Shinozaki,K. (2000) Various abiotic stresses rapidly activate *Arabidopsis* MAP kinases ATMPK4 and ATMPK6. *Plant J.*, **24**, 655–665.

13. Asai,T., Tena,G., Plotnikova,J., Willman,M.R., Chiu,W.L., Gomez-Gomez,L., Boller,T., Asubel,F.M. and Sheen,J. (2002) MAP kinase signaling cascade in *Arabidopsis* innate immunity. *Nature*, **415**, 977–983.
14. Mishra,N.S., Tuteja,R. and Tuteja,N. (2006) Signaling through MAP kinase networks in plants. *Arch. Biochem. Biophys.*, **452**, 55–68.
15. Droillard,M.J., Boudsoq,M., Barbier-Brygoo,H. and Lauriere,C. (2002) Different protein kinase families are activated by osmotic stresses in *Arabidopsis thaliana* cell suspensions. Involvement of the MAP kinases AtMPK3 and AtMPK6. *FEBS Lett.*, **527**, 43–50.
16. Gudesblat,G.E., Iusem,N.D. and Morris,P.C. (2007) Guard cell-specific inhibition of *Arabidopsis MPK3* expression causes abnormal stomatal responses to abscisic acid and hydrogen peroxide. *New Phytol.*, **173**, 713–721.
17. Xing,Y., Jia,W. and Zhang,J. (2007) AtMEK1 mediates stress-induced gene expression of CAT1 catalase by triggering H_2O_2 production in Arabidopsis. *J. Exp. Bot.*, **58**, 2969–2981.
18. Link,V., Sinha,A.K., Vashista,P., Hofmann,M.G., Proels,R.K., Ehness,R. and Roitsch,T. (2002) A heat-activated MAP kinase in tomato: a possible regulator of the heat stress response. *FEBS Lett.*, **531**, 179–183.
19. Kersten,B., Agrawal,G.K., Durek,P., Neigenfind,J., Schulze,W., Walther,D. and Rakwal,R. (2009) Plant phosphoproteomics: an update. *Proteomics*, **9**, 964–988.
20. Popescu,S.C., Popescu,G.V., Bachan,S., Zhang,Z., Gerstein,M., Snyder,M. and Dinesh-Kumar,S.P. (2009) MAPK target networks in Arabidopsis thaliana revealed using functional protein microarrays. *Genes Dev.*, **23**, 80–92.
21. Liu,Y. and Zhang,S. (2004) Phosphorylation of 1-aminocyclopropane-1-carboxylic acid synthase by MPK6, a stress-responsive mitogen-activated protein kinase, induces ethylene biosynthesis in Arabidopsis. *Plant Cell*, **16**, 3386–3399.
22. Nguyen,X.C., Kim,S.H., Lee,K., Kim,K.E., Liu,X.M., Han,H.J., Hoang,M.H., Lee,S.W., Hong,J.C., Moon,Y.H. and Chung,W.S. (2012) Identification of a C_2H_2-type zinc finger transcription factor (ZAT10) from *Arabidopsis* as a substrate of MAP kinase. *Plant Cell Rep.*, **31**, 737–745.
23. Agarwal,M., Hao,Y., Kapoor,A., Dong,C.H., Fujii,H., Zheng,X. and Zhu,J.K. (2006) A R2R3 type MYB transcription factor is involved in the cold regulation of CBF genes and in acquired freezing tolerance. *J. Biol. Chem.*, **281**, 37636–37645.
24. Jiang,Y. and Deyholos,M.K. (2006) Comprehensive transcriptional profiling of NaCl-stressed Arabidopsis roots reveals novel classes of responsive genes. *BMC Plant Biol.*, **6**, 6–25.
25. Murashige,T. and Skoog,F. (1962) A revised medium for rapid growth and bioassays with tobacco tissue cultures. *Plant Physiol.*, **15**, 473–497.
26. Chen,H., Zou,Y., Shang,Y., Lin,H., Wang,Y., Cai,R., Tang,X. and Zhou,J.M. (2008) Firefly luciferase complementation imaging assay for protein-protein interactions in plants. *Plant Physiol.*, **146**, 368–376.
27. Koncz,C. and Schell,J. (1986) The promoter of TL-DNA gene 5 controls the tissue-specific expression of chimaeric genes carried by a novel type of Agrobacterium binary vector. *Mol. Gen. Genet.* **204**, 383–396.
28. Bundock,P., den Dulk-Ras,A., Beijersbergen,A. and Hooykaas,P.J. (1995) Transkingdom T-DNA transfer from *Agrobacterium tumefaciens* to *Saccharomyces cerevisiae*. *EMBO J.*, **14**, 3206–3214.
29. Lee,K., Kye,M., Jang,J.S., Lee,O.J., Kim,T. and Lim,D. (2004) Proteomic analysis revealed a strong association of a high level of alpha1-antitrypsin in gastric juice with gastric cancer. *Proteomics*, **4**, 3343–3352.
30. Zhang,S. and Klessig,D.F. (1997) Salicylic acid activates a 48-kD MAP kinase in tobacco. *Plant Cell*, **9**, 809–824.
31. Sundaresan,V., Springer,P., Volpe,T., Haward,S., Jones,J.D., Dean,C., Ma,H. and Martienssen,R. (1995) Patterns of gene action in plant development revealed by enhancer trap and gene trap transposable elements. *Genes Dev.* **9**, 1797–17810.
32. Sheen,J. (1996) Ca^{2+}-dependent protein kinases and stress signal transduction in plants. *Science*, **274**, 1900–1902.
33. Kim,H.S., Park,B.O., Yoo,J.H., Jung,M.S., Lee,S.M., Han,H.J., Kim,K.E., Kim,S.H., Lim,C.O., Yun,D.J. *et al.* (2007) Identification of a calmodulin-binding NAC protein as a transcriptional repressor in Arabidopsis. *J. Biol. Chem.*, **282**, 36292–36302.
34. Raghothama,K.G., Maggio,A., Narasimhan,M.L., Kononowicz,A.K., Wang,G., D'Urzo,M.P., Hasegawa,P.M. and Bressan,R.A. (1997) Tissue-specific activation of the osmotin gene by ABA, C2H4 and NaCl involves the same promoter region. *Plant Mol. Biol.*, **32**, 393–404.
35. Clough,S.J. and Bent,A.F. (1998) Floral dip: a simplified method for *Agrobacterium*-mediated transformation of *Arabidopsis thaliana*. *Plant J.*, **16**, 735–743.
36. Ausubel,F.M., Brent,R., Kingston,R.E., Moore,D.D., Seidman,J.G., Smith,J.A. and Struhl,K. (1989) *Current Protocols in Molecular Biology*. Greene PublishingAssociates/Wiley Interscience, NY.
37. Ishitani,M., Xiong,L., Le,H., Stevenso,B. and Zhu,J.K. (1998) *HOS1*, a genetic locus involved in cold-responsive gene expression in Arabidopsis. *Plant Cell*, **10**, 1151–1161.
38. Mészáros,T., Helfer,A., Hatzimasoura,E., Magyar,Z., Serazetdinova,L., Rios,G., Bardóczy,V., Teige,M., Koncz,C., Peck,S. *et al.* (2006) The Arabidopsis MAP kinase kinase MKK1 participates in defence responses to the bacterial elicitor flagellin. *Plant J.*, **48**, 485–498.
39. Rodriguez,M.C., Petersen,M. and Mundy,J. (2010) Mitogen-activated protein kinase signaling in plants. *Annu. Rev. Plant Biol.*, **61**, 621–649.
40. Jin,H. and Martin,C. (1999) Multifunctionality and diversity within the plant *MYB*-gene family. *Plant Mol. Biol.*, **41**, 577–585.
41. Stracke,R., Werber,M. and Weisshaar,B. (2001) The *R2R3-MYB gene* family in *Arabidopsis thaliana*. *Curr. Opin. Plant Biol.*, **4**, 447–456.
42. Araki,S., Ito,M., Soyano,T., Nishihama,R. and Machida,Y. (2004) Mitotic cyclins stimulate the activity of c-Myb-like factors for transactivation of G2/M phase-specific genes in tobacco. *J. Biol. Chem.*, **279**, 32979–32988.
43. Haga,N., Kato,K., Murase,M., Araki,S., Kubo,M., Demura,T., Suzuki,K., Müller,I., Voss,U., Jürgens,G. *et al.* (2007) R1R2R3-Myb proteins positively regulate cytokinesis through activation of *KNOLLE* transcription in *Arabidopsis thaliana*. *Development*, **134**, 1101–1110.
44. Hoang,M.H., Nguyen,X.C., Lee,K., Kwon,Y.S., Pham,H.T., Park,H.C., Yun,D.J., Lim,C.O. and Chung,W.S. (2012) Phosphorylation by AtMPK6 is required for the biological function of AtMYB41 in Arabidopsis. *Biochem. Biophys. Res. Commun.*, **422**, 181–186.
45. Nguyen,X.C., Hoang,M.H., Kim,H.S., Lee,K., Liu,X.M., Kim,S.H., Bahk,S., Park,H.C. and Chung,W.S. (2012) Phosphorylation of the transcriptional regulator MYB44 by mitogen activated protein kinase regulates Arabidopsis seed germination. *Biochem. Biophys. Res. Commun.*, **423**, 703–708.
46. Nguyen,X.C., Kim,S.H., Hussain,S., An,J., Yoo,Y., Han,H.J., Yoo,J.S., Lim,C.O., Yun,D.J. and Chung,W.S. (2016) A positive transcription factor in osmotic stress tolerance, ZAT10, is regulated by MAP kinases in Arabidopsis. *J. Plant Biol.* **59**, 55–61.
47. Miglarese,M.R., Richardson,A.F., Aziz,N. and Bender,T.P. (1996) Differential regulation of c-myb-induced transcription activation by a phosphorylation site in the negative regulatory domain. *J. Biol. Chem.*, **271**, 22697–22705.
48. Bessa,M., Saville,M.K. and Watson,R.J. (2001) Inhibition of cyclin A/Cdk2 phosphorylation impairs B-Myb transactivation function without affecting interactions with DNA or the CBP coactivator. *Oncogene*, **20**, 3376–3386.
49. Johnson,L.R., Johnson,T.K., Desler,M., Luster,T.A., Nowling,T., Lewis,R.E. and Rizzino,A. (2002) Effects of B-Myb on gene ttranscription: PHSOPHORYLATION-DEPENDENT ACTIVITY AND ACETYLATION BY p300. *J. Biol. Chem.*, **277**, 4088–4097.
50. Li,X. and McDonnell,D.P. (2002) The transcription factor B-myb is maintained in an inhibited state in target cells through its interaction with the nuclear corepressors N-CoR and SMRT. *Mol. Cell. Biol.*, **22**, 3663–3673.
51. Schubert,S., Horstmann,S., Bartusel,T. and Klempnauer,K.H. (2004) The cooperation of B-Myb with the coactivator p300 is orchestrated by cyclins A and D1. *Oncogene*, **23**, 1392–1404.
52. Dubos,C., Stracke,R., Grotewold,E., Weisshaar,B., Martin,C. and Lepiniec,L. (2010) MYB transcription factors in *Arabidopsis*. *Trends Plant Sci.*, **15**, 573–581.
53. Yang,S.H., Sharrocks,A.D. and Whitmarsh,A.J. (2003) Transcriptional regulation by the MAP kinase signaling cascades. *Gene*, **320**, 3–21.

54. Moyano,E., Martínez-Garcia,J.F. and Martin,C. (1996) Apparent redundancy in *myb* gene function provides gearing for the control of flavonoid biosynthesis in antirrhinum flowers. *Plant Cell*, **8**, 1519–1532.
55. Morse,A.M., Whetten,R.W., Dubos,C. and Campbell,M.M. (2009) Post-translational modification of an R2R3-MYB transcription factor by a MAP Kinase during xylem development. *New Phytol.*, **183**, 1001–1013.
56. Fowler,S. and Thomashow,M.F. (2002) Arabidopsis transcriptome profiling indicates that multiple regulatory pathways are activated during cold acclimation in addition to the CBF cold response pathway. *Plant Cell*, **14**, 1675–1690.
57. Lee,H., Xiong,L., Gong,Z., Ishitani,M., Stevenson,B. and Zhu,J.K. (2001) The *Arabidopsis HOS1* gene negatively regulates cold signal transduction and encodes a RING finger protein that displays cold-regulated nucleo-cytoplasmic partitioning. *Genes Dev.*, **15**, 912–924.
58. Gilmour,S.J., Fowler,S.G. and Thomashow,M.F. (2004) Arabidopsis transcriptional activators CBF1, CBF2, and CBF3 have matching functional activities. *Plant Mol. Biol.*, **54**, 767–781.
59. Dong,C.H., Agarwal,M., Zhang,Y., Xie,Q. and Zhu,J.K. (2006) The negative regulator of plant cold responses, HOS1, is a RING E3 ligase that mediates the ubiquitination and degradation of ICE1. *Proc. Natl. Acad. Sci. U.S.A.*, **103**, 8281–8286.
60. Miura,K., Jin,J.B., Lee,J., Yoo,C.Y., Stirm,V., Miura,T., Ashworth,E.N., Bressan,R.A., Yun,D.J. and Hasegawa,P.M. (2007) SIZ1-mediated sumoylation of ICE1 controls *CBF3/DREB1A* expression and freezing tolerance in *Arabidopsis*. *Plant Cell*, **19**, 1403–1414.